

Synthesis and properties of *c*-axis oriented epitaxial MgB₂ thin films

S. D. Bu, D. M. Kim, J. H. Choi, J. Giencke, E. E. Hellstrom, D. C. Larbalestier, S. Patnaik, L. Cooley, and C. B. Eom^{a)}

Department of Materials Science and Engineering, and Applied Superconductivity Center, University of Wisconsin-Madison, Madison, Wisconsin 53706

J. Lettieri and D. G. Schlom

Department of Materials Science and Engineering, Pennsylvania State University, University Park, Pennsylvania 16802

W. Tian and X. Q. Pan

Department of Materials Science and Engineering, University of Michigan-Ann Arbor, Ann Arbor, Michigan 48109

(Received 1 April 2002; accepted for publication 26 June 2002)

We report the growth and properties of epitaxial MgB₂ thin films on (0001) Al₂O₃ substrates. The MgB₂ thin films were prepared by depositing boron films via radio-frequency (rf) magnetron sputtering, followed by a postdeposition anneal at 850 °C in magnesium vapor. X-ray diffraction and cross-sectional transmission electron microscopy reveal that the epitaxial MgB₂ films are oriented with their *c*-axis normal to the (0001) Al₂O₃ substrate with a 30° rotation in the (0001) plane with respect to the substrate. The critical temperature was found to be 35 K and the anisotropy ratio, $H_{c2}^{\parallel}/H_{c2}^{\perp}$, was about 3 at 25 K. The critical current densities at 4.2 and 20 K (at 1 T perpendicular magnetic field) are 5×10^6 and 1×10^6 A/cm², respectively. The controlled growth of epitaxial MgB₂ thin films opens a new avenue in both understanding superconductivity in MgB₂ and technological applications. © 2002 American Institute of Physics. [DOI: 10.1063/1.1504490]

The discovery of superconductivity at 39 K in MgB₂¹ offers the possibility of a new class of high-speed superconducting electronic devices due to its favorable combination of higher critical temperature than conventional BCS superconductors and a symmetric order parameter (unlike HTS). It also stimulated a flurry of activity to explore the phenomenology and basic mechanism of superconductivity in this surprising material. MgB₂ possesses a number of attractive properties, including strongly coupled grain boundaries.² Several unusual phenomena, such as temperature-dependent electronic anisotropy³ and multiple superconducting gap structures,^{4,5} appear to distinguish MgB₂ from a conventional BCS superconductor, and remain to be explained.

A critical step for studying both intrinsic superconducting properties and the possibility of superconducting devices based on MgB₂ is the controlled growth of high quality epitaxial MgB₂ thin film heterostructures. The growth of MgB₂ films by means of both *in situ* and *ex situ* processes has been demonstrated,^{6–15} including (0001) fiber-textured MgB₂ films.⁷ Kang *et al.* reported the growth of both *c*-axis and (101)-oriented MgB₂ epitaxial thin films on (1 $\bar{1}$ 02) Al₂O₃ and (100) SrTiO₃ substrates.⁶ However, the reported x-ray data do not show in-plane epitaxy, and there is no clear relationship between the MgB₂ film orientation and the orientation of the substrate, which must be present if epitaxial control over the film growth had been attained.

In this letter, we report the growth and properties of epitaxial MgB₂ thin films on (0001) Al₂O₃ substrates. In the time since we first reported the epitaxial growth of MgB₂ on thin films (0001) Al₂O₃,¹³ two other groups have also

achieved its epitaxial growth.^{14,15} Although MgB₂ has a mismatch with Al₂O₃ of ~23% along the [11 $\bar{2}$ 0] axis, which is unfavorable for epitaxial growth, a 30° in-plane rotation of the [11 $\bar{2}$ 0] direction of the MgB₂ film with respect to the substrate results in a parallel orientation of [11 $\bar{2}$ 0] MgB₂ and [10 $\bar{1}$ 0] Al₂O₃. This provides a lattice mismatch of ~11%.

The MgB₂ thin films were prepared by depositing boron via rf magnetron sputtering, followed by a postdeposition anneal at 850 °C in the presence of magnesium vapor. Deposition was carried out at 5 mTorr argon at 500 °C using a pure boron target. The thickness of the boron films was 230 nm. The films were annealed in an evacuated quartz tube using a tantalum envelope for 5 h. The quartz tube was filled with 7–10 Torr of argon gas after evacuation to reduce the Mg loss. The film thickness increased by a factor of 1.8 during the annealing, resulting in a final thickness of 400 nm, which was confirmed by cross-sectional transmission electron microscopy (TEM). Atomic force microscopy (AFM) imaging revealed a smooth surface morphology with a rms roughness of ~3 nm. The chemical composition was obtained using wavelength dispersive x-ray spectroscopy (WDS), showing a Mg:B:O:C atomic ratio of 34.1 : 58.4 : 4.3 : 3.2, respectively. By assuming that the carbon resides on boron sites and oxygen consumes magnesium to form MgO, the Mg:B ratio of film 1 was found to be 1:2.07, which is close to the MgB₂ stoichiometry.

The epitaxial relationships and the crystalline quality of the MgB₂ thin films were assessed by four-circle x-ray diffraction. Figure 1(a) shows a θ - 2θ scan of an epitaxial MgB₂ thin film grown on a (0001) Al₂O₃ substrate. The only substantial MgB₂ peaks are the 0001 and 0002 reflections, which clearly shows that the MgB₂ is oriented with its *c*-axis

^{a)}Author to whom correspondence should be addressed; electronic mail: eom@engr.wisc.edu

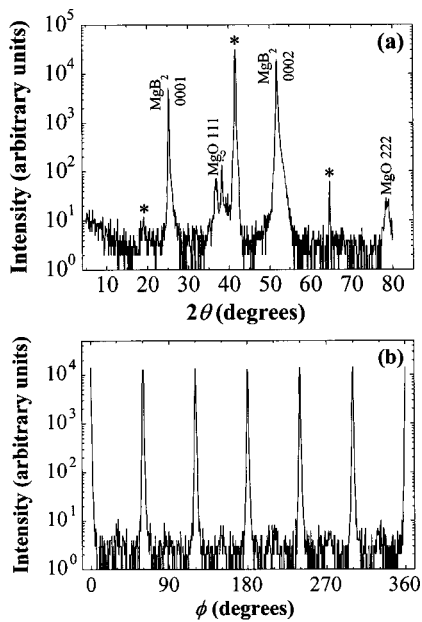


FIG. 1. X-ray diffraction scans of an epitaxial MgB_2 thin film grown on a (0001) Al_2O_3 substrate (a) θ - 2θ scan and (b) ϕ scan of the $10\bar{1}1$ MgB_2 reflection. The Al_2O_3 substrate peaks are marked as *. $\phi=0^\circ$ is aligned to be parallel to the $[11\bar{2}0]$ in-plane direction of the Al_2O_3 substrate. The FWHM of the 0002 MgB_2 peak is 0.28° in 2θ and 0.54° in ω (rocking curve). These scans indicate that the lattice constants of this MgB_2 film (film 2) are $a=3.08\pm 0.02 \text{ \AA}$ and $c=3.52\pm 0.01 \text{ \AA}$.

normal to the substrate. The rocking curve full width at half maximum (FWHM) of the 0002 MgB_2 reflection is 0.54° , which indicates that the crystalline quality of the film is good. We also investigated the in-plane texture of the film by scanning an off-axis peak. Figure 1(b) shows the azimuthal ϕ scan of the MgB_2 $10\bar{1}1$ reflection. The significant intensities every 60° of this reflection confirm that the film contains a single hexagonal texture in the film plane. Furthermore, the MgB_2 reflections are rotated 30° in the basal plane with respect to the Al_2O_3 lattice, resulting in a relationship between the substrate and MgB_2 film of $[11\bar{2}0]\text{MgB}_2\parallel[10\bar{1}0]\text{Al}_2\text{O}_3$. The measured FWHM of the azimuthal ϕ scan of the $10\bar{1}1$ reflection is 1.0° . The c -axis lattice parameter determined from normal θ - 2θ scans is $3.52\pm 0.01 \text{ \AA}$, which is the same as the bulk value.¹

The microstructure has been studied by cross-sectional TEM. Figure 2(a) is a low magnification bright field TEM image of a 4000 \AA thick MgB_2 film grown on a (0001) Al_2O_3 substrate. Figures 2(b) and 2(c) are the selected-area electron diffraction (SAED) pattern taken from the film and the substrate, respectively. Epitaxial growth of MgB_2 is evident and no grain boundaries are seen in the film. The high-resolution TEM (HRTEM) image in Fig. 2(d) shows distinct interface layers of MgAl_2O_4 and MgO between the MgB_2 and Al_2O_3 . The HRTEM image clearly shows that both MgAl_2O_4 and MgO grow epitaxially on the (0001) Al_2O_3 , with an orientation relationship of $(111)[1\bar{1}0]\text{MgO}\parallel(111)[1\bar{1}0]\text{MgAl}_2\text{O}_4\parallel(0001)[10\bar{1}0]\text{Al}_2\text{O}_3$. Additional details of TEM studies are given elsewhere.¹⁶

The transition temperature was measured with a SQUID magnetometer in a magnetic field of 5 mT, applied parallel to the film surface. Figure 3 shows an extremely sharp transition with onset at 35 K with full shielding. The 10% to 90% width of the inductive transition is $\sim 1 \text{ K}$, which is similar to

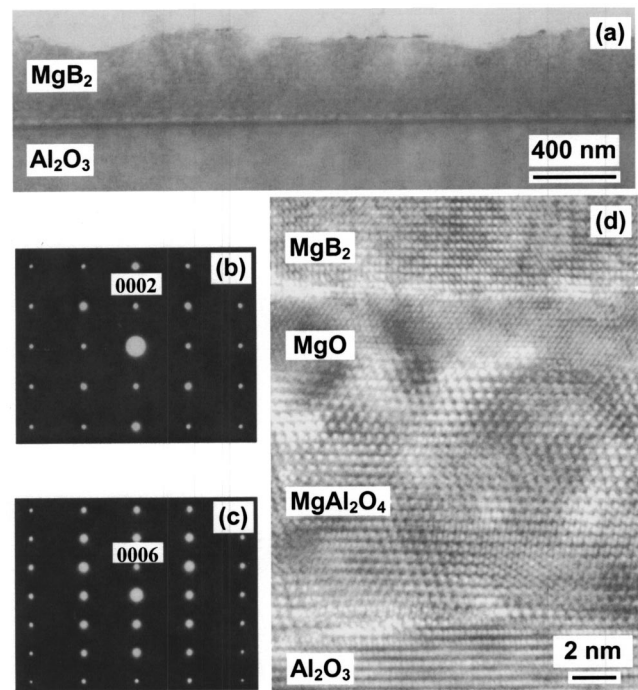


FIG. 2. (a) Bright-field cross-sectional TEM image of a 4000 \AA thick MgB_2 thin film grown on a (0001) Al_2O_3 substrate, (b) SAED of MgB_2 along the $[11\bar{2}0]$ zone axis, (c) SAED of Al_2O_3 substrate along the $[10\bar{1}0]$ zone axis, and (d) cross-sectional HRTEM micrograph of an epitaxial MgB_2 thin film near the (0001) Al_2O_3 substrate.

inductive transitions for the best bulk and single crystal samples made so far.¹⁷

The resistance was measured by a standard four-point technique in magnetic fields up to 9 T as a function of temperature. Figure 4 shows the zero field resistive transition, which indicates $\rho(40 \text{ K})=6.5 \mu\Omega \text{ cm}$ and a residual resistance ratio (RRR) of ~ 2 . We also measured the infield transitions for field applied parallel to the c axis and to the ab plane of the film. The infield resistive transitions exhibit very little broadening up to the highest field measured (9 T), unlike our earlier measurements on fiber-textured films.³ The upper critical field was defined for parallel (H_{c2}^{\parallel}) and perpendicular (H_{c2}^{\perp}) fields by extrapolating the steep part of the transition to the normal state resistance.³ The inset to Fig. 4 shows the upper critical field versus temperature. The anisotropy ratio, $H_{c2}^{\parallel}/H_{c2}^{\perp}$, is about 3 at 25 K, rather greater than film^{3,18} and single crystal values.¹⁷ At low temperatures, the nearly parallel trends and similar slopes of $H_{c2}^{\parallel}(T)$ and $H_{c2}^{\perp}(T)$ suggest decreasing anisotropy with decreasing temperature, a trend which is opposite to some recent data.^{19,20} It

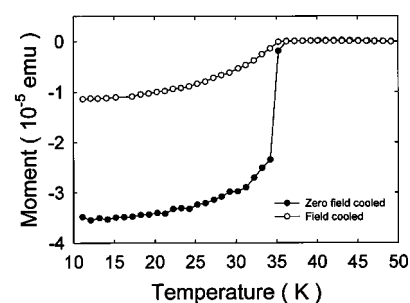


FIG. 3. T_c data obtained with a SQUID magnetometer utilizing a 5 mT magnetic field applied parallel to the film surface.

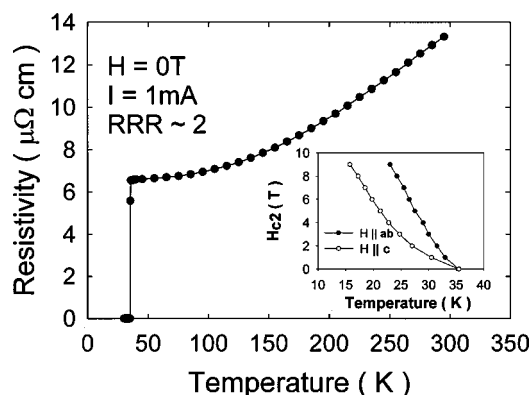


FIG. 4. Resistivity vs. temperature of MgB₂ thin film. The inset shows the H_{c2} for fields applied parallel and perpendicular to the crystal axes.

is clear that there is as yet no convergence on what the upper critical field anisotropy of MgB₂ is.

The critical current density, J_c , was determined by magnetization measurements using a vibrating sample magnetometer in the field range of 0–12 T. Figure 5 shows J_c vs. magnetic field at 4.2 and 20 K in a perpendicular magnetic field. To estimate J_c , we used the standard expression for the critical state of a thin film with rectangular area,²¹ $J_c = 2\Delta M(12b)/(3b-d)d$, where $b=4.5$ mm and $d=3.0$ mm are the film dimensions and ΔM is the total magnetization hysteresis measured from the field increasing and field decreasing branches of the magnetization curve. This analysis yields J_c values of 4.5×10^6 A/cm² at 4.2 K and 1 T, and 1×10^6 A/cm² at 20 K and 1 T. These values contrast the almost reversible behavior of bulk single crystals¹⁴ and are significantly larger than the values obtained from polycrystalline bulk forms of MgB₂,^{2,22,23} where grain boundary flux pinning is often thought to be operating. In this case grain boundaries cannot be responsible for the flux pinning, but it is evidently still very strong. We assume that some site interchange disorders must be contributing to the flux pinning.

In conclusion, we have demonstrated the growth of epitaxial MgB₂ films with high crystalline quality and high J_c . Although the films are epitaxial, the properties are distinctively different from bulk single crystals in terms of their very strong flux pinning and suppressed T_c . We attribute this to alloying of the MgB₂ film by impurity atoms or some other defects. The growth of epitaxial MgB₂ thin films with

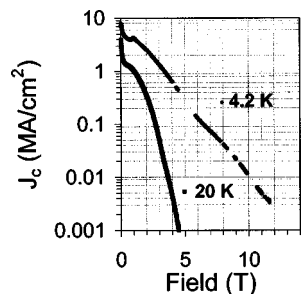


FIG. 5. Critical current density vs magnetic field measured using a vibrating sample magnetometer at 4.2 and 20 K in a perpendicular magnetic field. Deviations below 1 T are associated with the lack of full flux penetration and actual J_c values are higher.

controlled orientations and properties opens a new avenue to understand the superconductivity in MgB₂ and potential applications for both electronic devices and high field magnets.

The work at the University of Wisconsin was supported by National Science Foundation through the MRSEC for Nanostructure Materials. The authors are grateful to A. Gurevich for discussions. X.Q.P. gratefully acknowledges the financial support of the National Science Foundation through Grant Nos. DMR 9875405 (CAREER) and DMR/IMR 9704175.

- ¹J. Nagamatsu, N. Nakagawa, T. Muranaka, Y. Zenitani, and J. Akimitsu, *Nature* (London) **410**, 63 (2001).
- ²D. C. Larbalestier, L. D. Cooley, M. O. Rikel, A. A. Polyanskii, J. Jiang, S. Patnaik, X. Y. Cai, D. M. Feldmann, A. Gurevich, A. A. Squitieri, M. T. Naus, C. B. Eom, E. E. Hellstrom, R. J. Cava, K. A. Regan, N. Rogado, M. A. Hayward, T. He, J. S. Slusky, P. Khalifah, K. Inumaru, and M. Haas, *Nature* (London) **410**, 186 (2001).
- ³S. Patnaik, L. D. Cooley, A. Gurevich, A. A. Polyanskii, J. Jing, X. Y. Cai, A. A. Squitieri, M. T. Naus, M. K. Lee, J. H. Choi, L. Belenky, S. D. Bu, J. Letteri, X. Song, D. G. Schlom, S. E. Babcock, C. B. Eom, E. E. Hellstrom, and D. C. Larbalestier, *Supercond. Sci. Technol.* **14**, 315 (2001).
- ⁴P. Szabo, P. Samuely, J. Kacmarcik, T. Klein, J. Marcus, D. Fruchart, S. Miraglia, C. Marcenat, and A. G. M. Jansen, *Phys. Rev. Lett.* **87**, 7005 (2001).
- ⁵F. Giubileo, D. Roditchev, W. Sacks, R. Lamy, D. X. Thanh, J. Klein, S. Miraglia, D. Fruchart, J. Marcus, and P. Monod, *Phys. Rev. Lett.* **87**, 7008 (2001).
- ⁶W. N. Kang, H. J. Kim, E. M. Choi, C. U. Jung, and S. L. Lee, *Science* **292**, 1521 (2001).
- ⁷C. B. Eom, M. K. Lee, J. H. Choi, L. J. Belenky, X. Song, L. D. Cooley, M. T. Naus, S. Patnaik, J. Jiang, M. Rikel, A. Polyanskii, A. Gurevich, X. Y. Cai, S. D. Bu, S. E. Babcock, E. E. Hellstrom, D. C. Larbalestier, N. Rogado, K. A. Regan, M. A. Hayward, T. He, J. S. Slusky, K. Inumaru, M. K. Haas, and R. J. Cava, *Nature* (London) **411**, 558 (2001).
- ⁸D. H. A. Blank, H. Hilgenkamp, A. Brinkman, D. Mijatovic, G. Rijnders, and H. Rogalla, *Appl. Phys. Lett.* **79**, 394 (2001).
- ⁹X. X. Xi, Y. Zhang, A. Soukiassian, J. Jones, J. Hotchkiss, Y. Zhong, C. O. Brubaker, Z.-K. Liu, J. Lettieri, D. G. Schlom, Y. F. Hu, E. Wertz, Q. Li, W. Tian, H. P. Sun, and X. Q. Pan, *Supercond. Sci. Technol.* **15**, 451 (2002).
- ¹⁰H. Y. Zhai, H. M. Christen, L. Zhang, A. Paranthaman, C. Cantoni, B. C. Sales, P. H. Fleming, D. K. Christen, and D. H. Lowndes, *J. Mater. Res.* **16**, 2759 (2001).
- ¹¹K. Ueda and M. Naito, *Appl. Phys. Lett.* **79**, 2046 (2001).
- ¹²J.-U. H. W. Jo, T. Ohnishi, A. F. Marshall, M. R. Beasley, and R. H. Hammond, Presented at the MRS Fall Meeting (2001).
- ¹³C. B. Eom *et al.*, presented at the MRS Fall Meeting (2001).
- ¹⁴A. Berenov, Z. Lockman, X. Qi, J. L. MacManus-Driscoll, Y. Bugoslavsky, L. F. Cohen, M.-H. Jo, N. A. Stelmashenko, V. N. Tsaneva, M. Kambara, N. Hari Babu, D. A. Cardwell, and M. G. Blamire, *Appl. Phys. Lett.* **79**, 4001 (2001).
- ¹⁵X. H. Zeng, A. V. Pogrebnyakov, A. Kotcharov, J. E. Jones, X. X. Xi, E. M. Lysczek, J. M. Redwing, S. Y. Xu, Qi Li, J. Lettieri, D. G. Schlom, W. Tian, X. Q. Pan, and Z. K. Liu, *Nature Materials* (to be published).
- ¹⁶W. Tian, X. Q. Pan, S. D. Bu, D. M. Kim, J. H. Choi, S. Patnaik, and C. B. Eom, *Appl. Phys. Lett.* **81**, 685 (2002).
- ¹⁷M. Xu, H. Kitazawa, Y. Takano, J. Ye, K. Nishida, H. Abe, A. Matsushita, N. Tsujii, and G. Kido, *Appl. Phys. Lett.* **79**, 2779 (2001).
- ¹⁸C. Buzea and T. Yamashita, *Supercond. Sci. Technol.* **14**, R115 (2001).
- ¹⁹S. L. Yu, E. Iltsev, K. Nakao, N. Chikumoto, S. Tajima, N. Koshizuka, and M. Murakami, *cond-mat/0201451*.
- ²⁰M. Angst, R. Puzniak, A. Wisniewski, J. Jun, S. M. Kazakov, J. Karpinski, J. Roos, and H. Keller, *Phys. Rev. Lett.* **88**, 167004 (2002).
- ²¹J. Evertts, *Concise Encyclopedia of Magnetic and Superconducting Materials* (Pergamon, New York, 1992), p. 99.
- ²²D. K. Finnemore, J. E. Ostenson, S. L. Bud'ko, G. Lapertot, and P. C. Canfield, *Phys. Rev. Lett.* **86**, 2420 (2001).
- ²³G. Grasso, A. Malagoli, C. Ferdeghini, S. Roncallo, V. Braccini, A. S. Siri, and M. R. Cimberle, *Appl. Phys. Lett.* **79**, 230 (2001).